

Mechanism for the Oxidation of Sulfides and Sulfoxides with Periodates: Reactivity of the Oxidizing Species

Ferenc Ruff,*^[a] Attila Fábián,^[a] Ödön Farkas,^[a] and Árpád Kucsman^[a]

Keywords: Oxidation / Sulfides / Sulfoxides / Iodine / Density functional calculations / Reaction mechanisms

DFT computations have been performed at different levels of theory to identify the mechanism for the oxidation of sulfides and sulfoxides with periodates. The periodate ion (IO_4^-), periodic acid (HIO_4) and their hydrated derivatives all oxidize sulfides to sulfoxides in one-step oxygen-transfer reactions and the relative reactivities are $\text{HIO}_4 \gg \text{H}_5\text{IO}_6 > \text{IO}_4^- > \text{H}_4\text{IO}_6^- \gg \text{H}_3\text{IO}_6^{2-}$. The hydration and dissociation equilibria of the periodates are shifted towards IO_4^- in neutral and moderately acidic solutions, and sulfides are oxidized mainly with IO_4^- under normal experimental conditions. The oxygen atoms of the periodates attack the sulfides perpendicularly to the plane of the C–S–C atoms and the S...O...I atoms are in a linear arrangement in the very early transition state (TS). The sulfides are the electron donors and periodates are the

electron acceptors in the reactions; the geometries of the TSs are determined by the overlap of the HOMO and the LUMO of the reactants. Other mechanisms can be ruled out because the attack of the sulfur atom of the substrate on the iodine atom of the reactants increases the energy of the system continuously very steeply as the S...I distance decreases. Experimentally derived ΔG^\ddagger values are in good agreement with the ΔG^\ddagger data computed for the oxygen-transfer mechanism. Sulfoxides are also oxidized to sulfones with IO_4^- in a one-step oxygen-transfer reaction, and the structures of the TSs and the ΔG^\ddagger data are similar to those obtained for the reactions of sulfides.

(© Wiley-VCH Verlag GmbH & Co. KGaA, 69451 Weinheim, Germany, 2009)

Introduction

Periodates are commonly used for oxidations in organic chemistry.^[1–4] Organic sulfides can be oxidized with NaIO_4 to sulfoxides under mild conditions.^[5–10] Earlier we studied the mechanism of this reaction by kinetic methods^[11] and came to the conclusion that the reaction involves the rate-determining one-step oxygen-atom transfer from the periodate ion to the sulfur atom of the sulfide ($1 + 6 \rightleftharpoons \text{TS } 8$, Scheme 1). On the basis of studies^[12,13] on the oxidation of thiolsulfinates with periodate, Oae^[14] supposed, however, that the oxidation of sulfides with periodate occurs by the rate-determining attack of sulfur on the central iodine atom of periodate ($1 + 6 \rightleftharpoons 7$, Scheme 1) and a subsequent ligand-coupling reaction of the supposed trigonal bipyramidal intermediate (7). On the other hand, Musker and co-workers^[15,16] proposed the formation of a mixed anhydride intermediate of sulfinic and iodic acids ($\text{RSO}-\text{IO}_3$) for the periodate oxidation of thiols and disulfides rather than the oxygen-transfer mechanism.

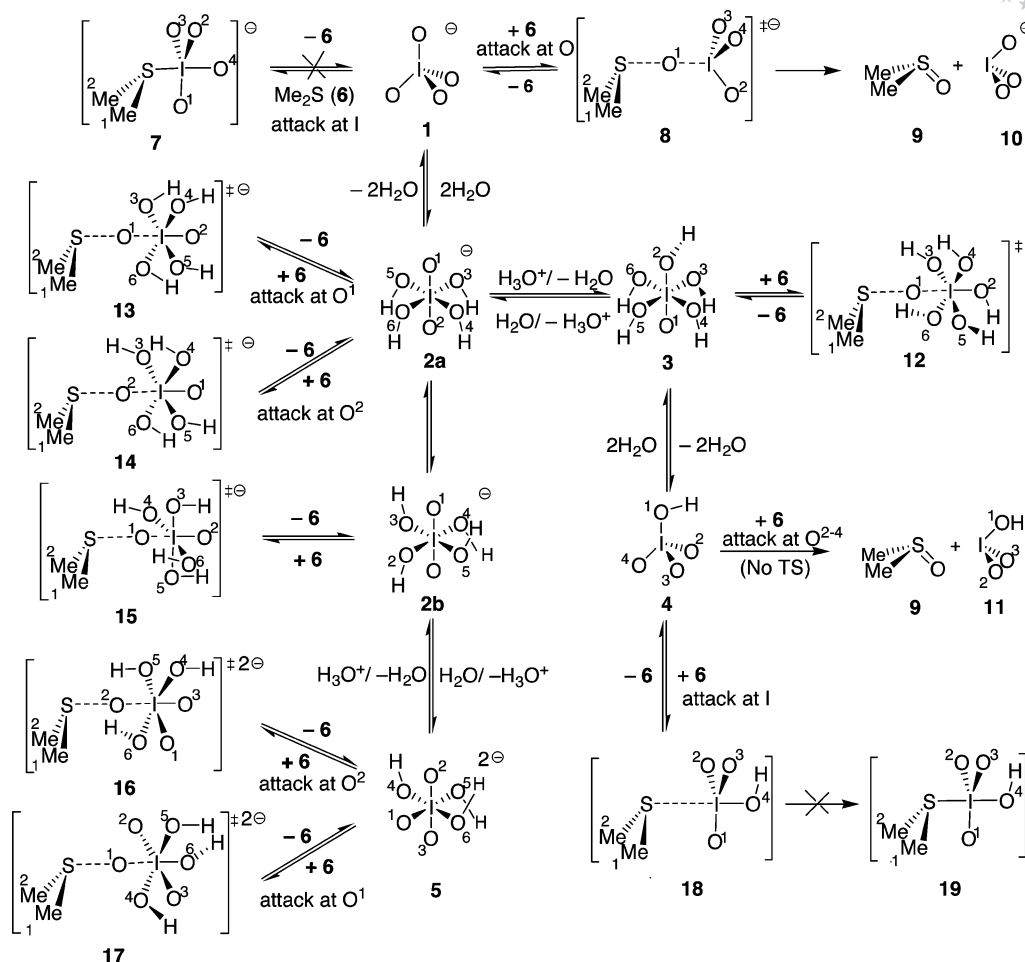
Four different mechanisms have been suggested^[17] for the oxidation of organic sulfides with reagents containing reactive oxygen atoms. a) The oxidation reactions of sulfides

and sulfoxides were suggested to proceed by a one-step oxygen-transfer mechanism in the reactions initiated by peroxides,^[17–20] percarboxylic acids,^[17,21–23] peroxomonophosphoric acid,^[24] as well as by permanganate^[25] and peroxomolybdate ions^[26] and several metal complexes.^[27–33] A mechanism involving oxygen-atom transfer steps has also been proposed for the periodate oxidation of the iodide ion.^[34–36] b) Mechanisms involving the nucleophilic addition of the sulfur atom of the sulfide to the central heteroatom of the oxidizing agents were proposed for the reactions of sulfides with pyridinium chlorochromate,^[37] iodosylbenzene diacetate^[38] and with complexes of permanganate^[39,40] and chromate ions.^[41–43] c) The oxidations of sulfides with peroxydisulfates,^[44] and peroxydiphosphates^[45] are thought to proceed via the formation of an acyloxysulfonium intermediate of sulfuric and phosphoric acids, respectively. d) In several reactions of sulfides with metal complexes and enzymes,^[17,46–51] evidence was found for mechanisms that involve single-electron transfer from the sulfide to the oxidizing agent and the rate-determining formation of the R_2S^{+} radical cation. The mechanism for the oxidation of sulfides and sulfoxides by dimethyldioxirane was found to change with the solvent. In less polar media the reactions were thought to proceed by a one-step oxygen transfer, whereas for reactions in a 20% (v/v) water in acetone mixture the formation of a sulfonium intermediate was proposed.^[52]

To ascertain the mechanism of the periodate oxidation of organic sulfides we have performed DFT computations on the previously proposed oxygen-transfer^[11] (mechanism

[a] Department of Organic Chemistry, Institute of Chemistry, L. Eötvös University
P.O. Box 32, 1518 Budapest 112, Hungary
Fax: +36-1-3722-620
E-mail: ruff@chem.elte.hu

Supporting information for this article is available on the WWW under <http://www.eurjoc.org> or from the author.



Scheme 1. Mechanisms for the oxidation of Me_2S (**6**) with the equilibrating species of periodates: IO_4^- (**1**), H_4IO_6^- (**2a**, **2b**), H_5IO_6 (**3**), HIO_4 (**4**) and $\text{H}_3\text{IO}_6^{2-}$ (**5**). TSs **12**–**17** are converted into products [TS **12** \rightarrow **9** + **11** + $2\text{H}_2\text{O}$; TS (**13**–**15**) \rightarrow **9** + **10** + $2\text{H}_2\text{O}$; TS (**16**, **17**) \rightarrow **9** + **10** + H_2O + HO^\cdot]. Formulae show the calculated structures of the species. The structural parameters are listed in Table 1 and Table S1 in the SI.

a) and nucleophilic addition^[14] mechanisms (mechanisms b). The formation of an acyloxysulfonium intermediate with periodate ($\text{R}_2\text{S}^+-\text{OIO}_3^{2-}$, mechanism c) and the electron transfer from sulfides to the periodate ion (R_2S^{+} , IO_4^{2-} , mechanisms d) were excluded because they involve large charge separations and the total energy of the intermediates with two negative charges on the periodate moieties are much higher than that of the reactants ($\Delta E = 284.4$ and $269.9 \text{ kJ mol}^{-1}$, respectively, cf. the Computational Methods Section).

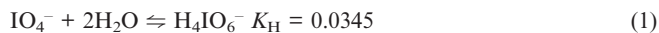
To validate the results of the computations, the obtained free energy of activation data were compared with the experimentally derived ΔG^\ddagger values, calculated from the rate constants of kinetic experiments.^[11] We previously found^[53–56] for several reactions that the computed and experimentally derived ΔG^\ddagger values are in acceptably good agreement; their deviations were found to be less than 10 kJ mol^{-1} . The agreement between the experimentally derived and computed ΔG^\ddagger data may be explained by two reasons. First, the effect of solvent polarity on reactivity (ΔG^\ddagger) can be computed by the DFT method by using the polarizable continuum model (PCM) of solvents. Secondly,

the contribution of the very fast rearrangement of solvent molecules to the experimentally derived ΔG^\ddagger is small. The rearrangement of solvent molecules influences, nevertheless, the experimentally derived ΔH^\ddagger and ΔS^\ddagger parameters; they decrease/increase together with increasing/decreasing solvation of the TS and may approximately compensate each other's changes according to the equation $\delta\Delta G^\ddagger = \delta\Delta H^\ddagger - T\delta\Delta S^\ddagger$. Therefore, in agreement with our earlier observations,^[53–56] although computed and experimentally derived ΔG^\ddagger values are in acceptable agreement with each other, the corresponding ΔH^\ddagger and ΔS^\ddagger data may be different because the rearrangement of the solvent molecules that occurs during the reaction cannot be computed with the applied methods.

Results and Discussion

Equilibria and Structures of the Periodate Oxidizing Species

The periodate ion (IO_4^-) and periodic acid (HIO_4) are hydrated^[57–60] in aqueous solution to provide H_4IO_6^- and H_5IO_6 , respectively [see Equations (1) and (2)].



The equilibrium constant for the dehydration of H_4IO_6^- ($K_{\text{D}} = 1/K_{\text{H}} = 29$ in water at 25 °C) was determined by spectroscopic methods.^[57,58] The hydration and dehydration of IO_4^- are rapid processes^[59] in spite of the large structural changes and the complexity of the reactions. Although equilibrium (1) is shifted^[57] towards IO_4^- , equilibrium (2) is shifted completely to the right.^[61,62] In aqueous solutions, HIO_4 exists exclusively in the hydrated form H_5IO_6 . Although HIO_4 is expected to be a very strong acid,^[57] like HClO_4 , its hydrated form H_5IO_6 ($\text{p}K_{\text{a}}^1 = 3.29$), and the anion H_4IO_6^- ($\text{p}K_{\text{a}}^2 = 8.31$) are weak acids.^[57,61–64] The apparent $\text{p}K_{\text{a}}$ values of H_5IO_6 and H_4IO_6^- depend on the hydration equilibrium^[57] and they are shifted^[11] to $\text{p}K_{\text{a}}^1 = 0.5$ and $\text{p}K_{\text{a}}^2 = 10.5$ in 50% (v/v) EtOH/ H_2O , as this medium is less able to hydrate periodates. In neutral and moderately acidic solutions, IO_4^- predominates; the concentrations of H_5IO_6 and $\text{H}_3\text{IO}_6^{2-}$ are high only at $\text{pH} < 2$ and $\text{pH} > 9$, respectively.

IO_4^- (1) and HIO_4 (4) have tetrahedral structures, whereas the hydrated species H_5IO_6 (3), H_4IO_6^- (2), and $\text{H}_3\text{IO}_6^{2-}$ (5) adopt octahedral geometries.^[61,62,65] IO_3^- (10) and HIO_3 (11) are pyramidal owing to the lone pair of the iodine (Scheme 1). The structural parameters, as calculated by the DFT method for the optimized structures (Tables S1–S5 and S8 in the Supporting Information), are similar to those obtained by X-ray diffraction for the salts of the corresponding species.^[62,65] The conformers **2a** and **2b** have been calculated for H_4IO_6^- . Four H atoms lie close to one of the axial oxygen atoms in **2a**, whereas two oppositely positioned H atoms are directed towards each of the axial oxygen atoms in **2b** (Scheme 1). The equilibrium **2a** \rightleftharpoons **2b** is shifted towards **2b** ($\Delta G^0 = -1.71 \text{ kJ mol}^{-1}$). The energies of other conformers of **2**, with different arrangements of the H atoms, lie between the energies of **2a** and **2b**.

Mechanism for the Oxidation of Me_2S and Me_2SO with Periodate

To clarify the mechanism for the periodate oxidation of organic sulfides calculations were performed by changing stepwise the distances between the sulfur atom of the sulfides and the oxygen or iodine atoms of the periodates. The calculations were performed at the DFT(B3LYP)/6-31G(d)-SDD level of theory, unless stated otherwise (cf. the Computational Methods Section). The total energy of the system increases steeply if the sulfur atom of Me_2S attacks the iodine atom of IO_4^- (**1** + **6** \rightleftharpoons **7**, Figure 1, Scheme 1). Structure **7** cannot be an intermediate of the reaction as it is not in a minimum on the relaxed potential energy curve at 2.37 Å, which is the calculated distance^[66,67] of a S–I single bond. Thus, a mechanism involving the formation of **7** and its conversion to products in subsequent ligand-coupling steps^[14] can be ruled out. On the other hand, the total energy of the system passes through a transition state (TS) if

the sulfur atom of Me_2S attacks one of the oxygen atoms of IO_4^- (**1** + **6** \rightleftharpoons TS **8** \rightarrow **9** + **10**, Figure 2, Scheme 1); the Me_2SO (**9**) and IO_3^- (**10**) products are formed with a considerable decrease of energy. In TS **8** the oxygen atom of IO_4^- approaches the sulfur atom at right angles to the plane of the Me_2S molecule [$\theta(\text{MeSO}^1) = 92.8^\circ$]. TS **8** has only one imaginary mode in which the oxygen atom passes from iodine to sulfur in a linear arrangement [$\theta(\text{SO}^1\text{I}) = 172.2^\circ$]. Ab initio calculations have shown^[68] that the oxygen-transfer reaction step also takes place at right angles [$\theta(\text{MeSO}) = 94.4^\circ$] to the plane of Me_2S when the oxidation proceeds with H_2O_2 .

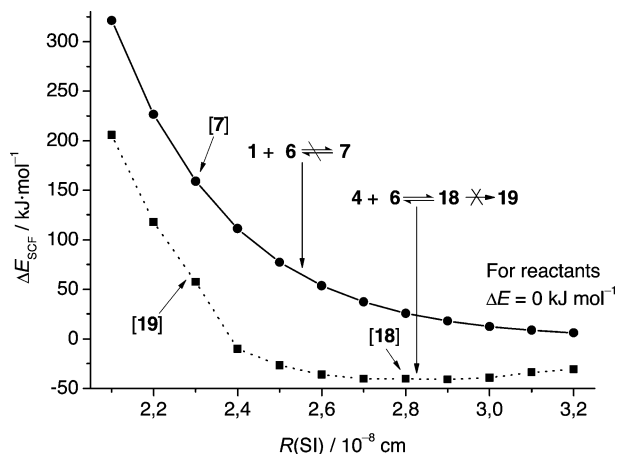


Figure 1. Relaxed potential energy curves for the attack of Me_2S (**6**) on the iodine atom of IO_4^- (**1** + **6** \rightleftharpoons **7**) and HIO_4 (**4** + **6** \rightleftharpoons **18** \rightleftharpoons **19**), as calculated for increasing S–I distance at the DFT(B3LYP)/6-31G(d)-SDD level of theory in water at 25 °C (Scheme 1).

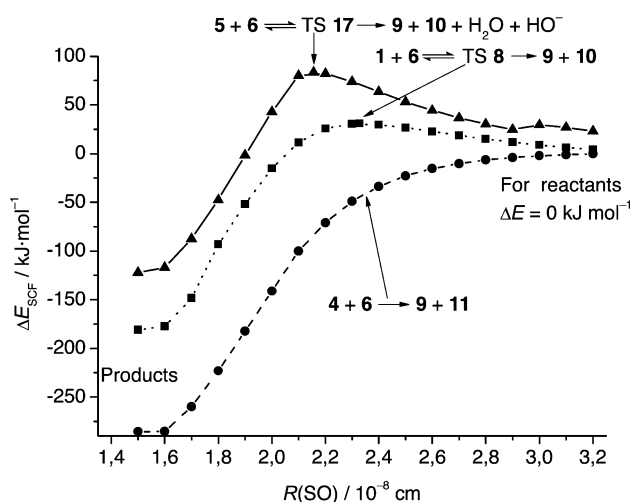


Figure 2. Relaxed potential energy curves for the attack of Me_2S (**6**) on the oxygen atoms of IO_4^- (**1** + **6** \rightleftharpoons TS **8** \rightarrow **9** + **10**), $\text{H}_3\text{IO}_6^{2-}$ (**5** + **6** \rightleftharpoons TS **17** \rightarrow **9** + **10** + H_2O + HO^-) and HIO_4 (**4** + **6** \rightarrow **9** + **11**), as calculated for increasing S–O distance at the DFT(B3LYP)/6-31G(d)-SDD level of theory in water at 25 °C (Scheme 1).

In the oxidation process the sulfide molecule is the electron donor and the periodate ion is the electron acceptor as electron-donating (e-d) substituents on the sulfides in-

crease the rate of the reactions.^[11] The sulfur atom is positively polarized in TS **8** [$Q(S) = 0.248$ a.u.], whereas the negative charge on the attacking oxygen atom of IO_4^- (**1**) is smaller [$Q(O^1) = -0.685$ a.u.] than that of the other three oxygen atoms in the periodate moiety [$Q(O^{2-4}) \approx -0.85$ a.u.] and smaller than that of IO_4^- [$Q(O) = -0.799$ a.u., Table 1 and Table S1]. Electrons are shifted from sulfur towards the oxygen atoms of the leaving IO_3^- during the reaction. The HOMO of Me_2S on the sulfur atom is perpendicular to the plane of the Me_2S molecule. The LUMO on the oxygen atoms of IO_4^- is on the opposite side of the I–O bond (Figure 3). Thus the geometry of the TS **8** is determined by the HOMO–LUMO interaction of the reactants.

Table 1. Free energies of activation (ΔG^\ddagger), bond lengths (R) and net Mulliken atomic charges (Q) for the TSs in the oxidation of Me_2S (**6**) and Me_2SO (**9**) with periodates (Scheme 1 and Scheme 2) and for the TSs in the oxygen-exchange reactions between Me_2S (**6**), Me_2SO (**9**), Me_2SO_2 (**21**), IO_4^- (**1**) and IO_3^- (**10**, Scheme 3), as computed at the DFT(B3LYP)/6-31G(d)-SDD level of theory in water at 25 °C.

Reaction	ΔG^\ddagger [kJ mol ⁻¹]	$R(SO^1)$ [Å]	$R(IO^1)$ [Å]	$Q(S)$ [a.u.]	$Q(O^1)$ [a.u.]	$Q(I)$ [a.u.]
1 1 + 6 \rightleftharpoons TS 8	78.2	2.327	1.977	0.248	-0.685	1.950
2 3 + 6 \rightleftharpoons TS 12	62.6	2.447	1.914	0.229	-0.746	2.267
3 2a + 6 \rightleftharpoons TS 13	90.0	2.304	1.994	0.235	-0.723	2.182
4 2a + 6 \rightleftharpoons TS 14	100.5	2.267	2.013	0.254	-0.750	2.140
5 2b + 6 \rightleftharpoons TS 15	94.3	2.269	2.017	0.255	-0.742	2.156
6 5 + 6 \rightleftharpoons TS 16	133.6	2.156	2.097	0.277	-0.736	1.937
7 5 + 6 \rightleftharpoons TS 17	176.8	2.032	2.164	0.332	-0.731	1.860
8 1 + 9 \rightleftharpoons TS 20	76.3	2.224	1.996	0.873	-0.707	1.973
9 6 + 9 \rightleftharpoons TS 22	240.6	2.027	–	0.314	-0.593	–
10 9 + 21 \rightleftharpoons TS 23	282.8	1.961	–	0.912	-0.641	–
11 1 + 10 \rightleftharpoons TS 24	81.7	–	2.150	–	-0.764	1.915

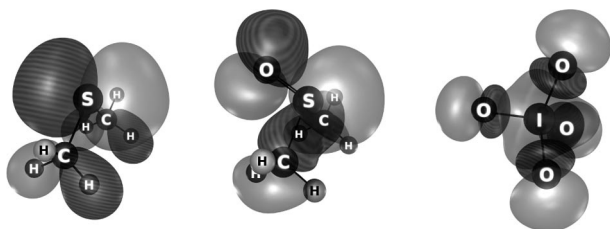


Figure 3. HOMOs of Me_2S (**6**) and Me_2SO (**9**) and LUMO of IO_4^- (**1**), as calculated at the DFT(B3LYP)/6-31G(d)-SDD level of theory in water at 25 °C. Dark grey represents positive signs and light grey represents the negative signs of the MOs (normally shown in red and green colors, respectively).

A free energy of activation of $\Delta G^\ddagger = 78.2$ kJ mol⁻¹ was computed for the reaction of Me_2S with IO_4^- (**1** + **6** \rightleftharpoons TS **8**, Scheme 1) at the DFT(B3LYP)/6-31G(d)-SDD level of theory in water (Table 1, Entry 1), and $\Delta G^\ddagger = 76.3$ kJ mol⁻¹ was obtained from the rate constants, as measured^[11] in 50% (v/v) EtOH/H₂O at 25 °C. We found previously^[53] that the given level of theory and the basis set can also be used to calculate ΔG^\ddagger values in S_N2 reactions involving MeI and ArNMe₂ in different solvents. Calculations were performed

earlier in the gas phase at a higher DFT(B3LYP)/6-311G(d,p)-SDD level of theory^[69] or by using the MP2 theory^[70] or the LANL2P2 basis set^[71] for the reactions of iodine or compounds containing an iodine atom, and the results were found to be in good agreement with the experimental data. Our calculations, performed with these and other higher basis sets for the reaction of Me_2S (**6**) with IO_4^- (**1**) in water, proved that diffuse functions, in general, had no affect, however, surprisingly, increasing the number of basis functions led to an increase in the barrier of the reaction (Table S7 in the SI). Nevertheless, we are convinced that the results calculated at the moderate DFT(B3LYP)/6-31G(d)-SDD level of theory can be used to obtain satisfactory information for ascertaining the mechanism of the studied reactions.

The reactivity of the periodate oxidizing species can be characterized by the free energies of activation, as calculated for the reactions proceeding with Me_2S . TSs similar to TS **8** are formed when Me_2S (**6**) attacks the oxygen atoms of hydrated periodates H_5IO_6 (**3** + **6** \rightleftharpoons TS **12**), $H_4IO_6^-$ (**2a** + **6** \rightleftharpoons TS **13** or **14**; **2b** + **6** \rightleftharpoons TS **15**) and $H_3IO_6^{2-}$ (**5** + **6** \rightleftharpoons TS **16** or **17**, Scheme 1). The structural parameters of the TSs are listed in Table 1 and Table S1 in the SI. The order HIO_4 (**4**) \gg H_5IO_6 (**3**) $>$ IO_4^- (**1**) $>$ $H_4IO_6^-$ (**2**) \gg $H_3IO_6^{2-}$ (**5**) shows that the reactivity decreases with hydration and with increasing negative charge on the oxidizing species (cf. the ΔG^\ddagger values in Table 1, Entries 1–7, and the ΔE^\ddagger data in Figure 2). Hydrogen atoms oriented towards the axial oxygen of the hydrated periodates hinder the attack of Me_2S (cf. ΔG^\ddagger values for the reactions of the conformers **2a** and **2b** in Table 1, Entries 3–5). The free energies of activation for the reactions of other conformers of **2** are between those of the reactions of **2a** and **2b**. The equatorial oxygen of the hydrated periodates is less reactive than the axial ones (cf. attack on O¹ and O² of the reactant **5**, Table 1, Entries 6 and 7). These results are in accord with earlier observations,^[65] which indicates that the oxidation potentials of solutions of periodates are the highest in acidic media and that they decrease with increasing pH.

Anhydrous HIO_4 (**4**) is a species of high energy and the most reactive of all the oxidizing periodates. In a non-aqueous medium it can oxidize Me_2S (**6**) in an extremely fast oxygen-transfer, with the sulfide attacking one of the non-protonated oxygen atoms in HIO_4 (**4**). This reaction has no energy of activation or TS because the total energy of the reacting species decreases continuously during the formation of the products (**4** + **6** \rightarrow **9** + **11**, Figure 2, Scheme 1). On the other hand, the attack of Me_2S on the iodine atom of HIO_4 is not favoured energetically. A complex (**18**) can be formed from Me_2S (**6**) and HIO_4 (**4**) in an energy minimum at a distance $R(S\cdots I) = 2.87$ Å (**4** + **6** \rightleftharpoons **18**, Figure 1; $\Delta E^\circ = -41.1$ kJ mol⁻¹, $\Delta G^\circ = 14.1$ kJ mol⁻¹, $K = 0.0034$). At distances $R(S\cdots I) < 2.5$ Å, however, the total energy of the system increases continuously (**18** \rightleftharpoons **19**, Figure 1, Scheme 1). As the calculated^[66,67] bond length for the S–I single bond in structure **19** is 2.37 Å, one may conclude that protonation of the periodate ion does not promote the formation of an intermediate with a S–I single bond. There-

Table 2. Total, strain and interaction energies (ΔE) and selected structural data (R , θ) for the intermediate species of the reactions of Me_2S with IO_4^- (**7** and **TS 8**) and Me_2S with HIO_4 (**4** + **6**, **18** and **19**), as calculated at the DFT(B3LYP)/6-31G(d)-SDD level of theory in water at 25 °C (Scheme 1).

Species	ΔE [kJ mol ⁻¹]	ΔE_{strain} [kJ mol ⁻¹]	ΔE_{int} [kJ mol ⁻¹]	$R(\text{SO})$ [Å]	$R(\text{SI})$ [Å]	$\theta(\text{O}^1\text{IO}^2)$ [°]	$\theta(\text{O}^2\text{IO}^3)$ [°]	$\theta(\text{O}^1\text{IO}^4)$ [°]
1 TS 8	30.63	31.48	-0.85	2.327	—	112.6 ^[a]	105.4 ^[a]	113.2 ^[a]
2 7 ^[b]	123.78	53.42	70.36	—	2.370	117.3 ^[a]	118.9 ^[a]	98.2 ^[a]
3 4 + 6 ^[c]	-43.89	358.81	-402.7	2.330	—	125.0 ^[d]	110.3 ^[d]	85.0 ^[e]
4 18	-41.21	293.30	-334.5	—	2.874	119.2 ^[d]	119.2 ^[d]	91.2 ^[e]
5 19 ^[b]	27.06	312.01	-284.9	—	2.370	119.5 ^[d]	119.9 ^[d]	89.7 ^[e]

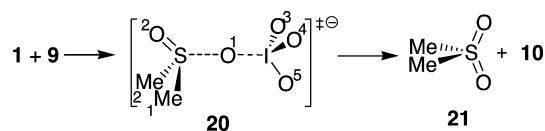
[a] $\theta(\text{OIO}) = 109.4^\circ$ for IO_4^- . [b] Data for the species with the distance $R(\text{SI}) = 2.37$ Å. [c] Data for the reacting species with the distance $R(\text{SO}^1) = 2.33$ Å. [d] $\theta(\text{O}^1\text{IO}^2) = 105.9^\circ$, $\theta(\text{O}^2\text{IO}^3) = 115.4^\circ$ for HIO_4 . [e] $\theta(\text{O}^1\text{IO}^4) = 97.3^\circ$ for HIO_4 .

fore, the mechanism^[14] involving the formation of the supposed intermediate **19** and the subsequent ligand-coupling steps may be ruled out.

To find the reason for the difference in the reactivities of IO_4^- (**1**) and HIO_4 (**4**), the “Activation Strain Analysis” proposed by Bickelhaupt^[72,73] was applied to the intermediates and TSs, which were taken into account in the reactions of these oxidizing species with Me_2S (**6**). The total energies of formation of the intermediates and TSs were broken down into strain and interaction components ($\Delta E = \Delta E_{\text{strain}} + \Delta E_{\text{int}}$). The strain energy was calculated from the total energy of the reactants, which adopt the same conformations as the intermediates or transition states. Both the strain and interaction energies of the supposed^[14] intermediate **7** are much higher than those of **TS 8** (Table 2, Entries 1 and 2). Therefore, the reaction of Me_2S (**6**) with IO_4^- (**1**) occurs via **TS 8**, with the attack of Me_2S on one of the oxygen atom of IO_4^- (Scheme 1). In the reaction of HIO_4 (**4**) and Me_2S (**6**), the approach of the reactants results in a large decrease in the interaction energy ($\Delta E_{\text{int}} \ll 0$) and in a large increase in the strain energy ($\Delta E_{\text{strain}} \gg 0$, Table 2, Entries 3–5). In the attack of Me_2S on the oxygen of HIO_4 (**4** + **6**) and in complex **18**, the strong interactions make possible a large distortion of the HIO_4 molecule, which manifests itself by a large change in the bond angles (compare the θ values given in Table 2 with those of the reactants HIO_4 and IO_4^-). The total energy ($\Delta E < 0$) decreases when Me_2S attacks the oxygen atom of HIO_4 (**4** + **6**, Figure 2) and on formation of complex **18** (Figure 1). The formation of the supposed^[14] intermediate **19**, however, proceeds with an increase in ΔE [Figure 1, $R(\text{S-I}) = 2.37$ Å] and therefore can be neglected.

IO_4^- oxidizes Me_2SO to Me_2SO_2 (**1** + **9** \rightleftharpoons **TS 20** \rightarrow **21** + **10**, Scheme 2). The structure of **TS 20** [$\theta(\text{MeSO}^1) = 99.0^\circ$, $\theta(\text{SO}^1\text{I}) = 168.8^\circ$] is similar to that of **TS 8** formed in the

reaction of Me_2S and IO_4^- . The orientation of the HOMO of Me_2SO is also quasi-perpendicular to the plane of the C–S–C atoms of the molecule (Figure 3). The ΔG^\ddagger values computed for the oxidations of Me_2S (**1** + **6** \rightleftharpoons **TS 8**) and Me_2SO (**1** + **9** \rightleftharpoons **TS 20**, Table 1, Entries 1 and 8) were approximately the same. It is well known that the rates of periodate oxidations of sulfides and sulfoxides are similar. Therefore sulfoxides must be prepared^[5–7,10] at a low temperature with an equivalent amount of IO_4^- to avoid the formation of sulfones.



Scheme 2. Mechanism for the oxidation of Me_2SO (**9**) with IO_4^- (**1**).

The calculated lengths of the $\text{S}\cdots\text{O}^1$ distances ($R_{\text{R}} \approx 2.25$ Å) in TSs **8** and **20** are much longer than those of the $\text{S}=\text{O}$ bonds ($R_{\text{O}} \approx 1.5$ Å) in Me_2SO (**9**) and Me_2SO_2 (**21**), but the $\text{I}\cdots\text{O}^1$ distances in TSs **8** and **20** are only slightly longer ($R_{\text{R}} \approx 1.98$ Å) than the $\text{I}-\text{O}$ bonds of IO_4^- ($R_{\text{O}} = 1.829$ Å, Table 3). The bond orders of $n \approx 0.33$ and $n \approx 0.73$ were calculated for the $\text{S}\cdots\text{O}$ and $\text{I}\cdots\text{O}$ bonds, respectively, in **TS 8** and **20** by the Pauling equation^[74] [Equation (3)], which indicates that very early TSs are formed in the oxidation reactions of Me_2S and Me_2SO with IO_4^- .

$$R - R_{\text{O}} = a \ln n \quad (3)$$

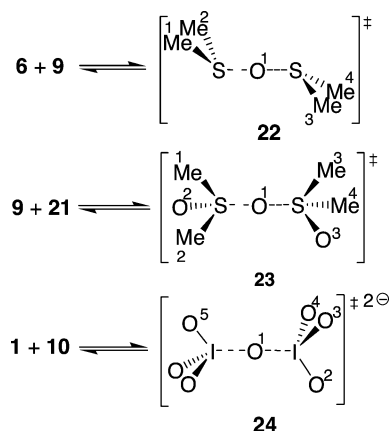
The a constants of the Pauling equation for the S–O and I–O bonds were obtained by using the calculated bond lengths of Me_2SO , Me_2SO_2 and IO_4^- (R_{O}) and those of the symmetric ($n = 0.5$) TSs **22–24** (R_{S}) of the oxygen-exchange

Table 3. Calculated bond orders (n)^[a] for the TSs **8** and **20** (Scheme 1 and Scheme 2) generated in the reactions of Me_2S (**6**) and Me_2SO (**9**) with IO_4^- (**1**).

Reaction	Bond	$R_{\text{S}}^{\text{[b,c]}}$ [Å]	$R_{\text{O}}^{\text{[c,d]}}$ [Å]	$a^{\text{[e]}}$	$R_{\text{R}}^{\text{[c,f]}}$ [Å]	n
1 + 6 \rightleftharpoons TS 8	SO	2.026 (22)	1.528 (9)	-0.7199	2.327 (8)	0.33
	IO	2.150 (24)	1.829 (1)	-0.4631	1.977 (8)	0.73
1 + 9 \rightleftharpoons TS 20	SO	1.961 (23)	1.478 (21)	-0.6968	2.224 (20)	0.34
	IO	2.150 (24)	1.829 (1)	-0.4631	1.996 (20)	0.70

[a] Bond orders were calculated according to Pauling^[74] [Equation (3)]. [b] Atomic distances were calculated for symmetric TSs ($n = 0.5$). [c] The number of the relevant species is given in parentheses. [d] Bond lengths calculated for the reactants. [e] Constants calculated by Equation (3). [f] Atomic distances calculated for the TSs.

reactions^[75] (Scheme 3). The bond orders were obtained by using the R_R bond lengths, as calculated for TSs **8** and **20** (Table 3).



Scheme 3. Structures of the symmetric TSs of the oxygen-exchange reactions between Me_2S (**6**) and Me_2SO (**9**), between Me_2SO (**9**) and Me_2SO_2 (**21**), and between IO_4^- (**1**) and IO_3^- (**10**).

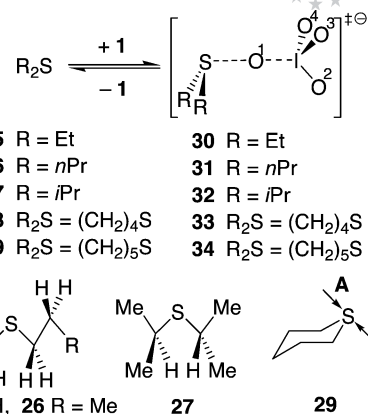
The reaction coordinates of the TSs depend on the reactivity of the oxidizing periodate species. The $Q(\text{S})$ charges on the sulfur atom and the $R(\text{O}^1\cdots\text{I})$ distances increase whereas the $R(\text{S}\cdots\text{O}^1)$ distances decrease in the TSs with increasing free energy of activation of the oxidations of Me_2S with different species of periodates (Table 1, Entries 1–9, Figure 2). The greater the ΔG^\ddagger value, the greater the reaction coordinate of the TS, so later TSs are formed with less reactive periodate species.

Reactions of Dialkyl Sulfides with IO_4^-

The experimentally derived ΔG^\ddagger data^[11] for the oxidations of dialkyl sulfides **6** and **25–27** with IO_4^- (Scheme 4, Table 4, Entries 1–4) can be correlated with the inductive (σ^*) and steric (E_s) substituent constants of the Taft equation^[76] [Equation (4), ΔG^\ddagger values are given in kJ mol^{-1}].

$$\Delta G^\ddagger(\text{exp}) = 6.94\sigma^* - 2.31E_s + 70.7 (r = 0.949, N = 4) \quad (4)$$

The electron-donating (e-d) effects of the alkyl groups ($\sigma^* < 0$) decrease the free energy of activation, whereas the increasing steric hindrance of the substituents ($E_s < 0$) increase the value. Experimental ΔG^\ddagger values are the mean of



Scheme 4. TSs **30–34** of the oxidation reactions of dialkyl sulfides **25–29** by IO_4^- (**1**). Conformations of dialkyl sulfides **25–27** and the directions of attack of IO_4^- (**1**) on thiane **29A** and **29B**.

data obtained for attack of periodate ions on sulfides from several directions. The σ^* and E_s substituent constants are calculated from the rate constants of several kinetic measurements,^[76] and this is the reason for their good correlation with the experimentally derived free energies of activation of the periodate oxidation of sulfides. ΔG^\ddagger data computed for the attack of IO_4^- on the most stable, planar conformation of dialkyl sulfide **6** and **25–27** (Scheme 4), do not correlate with the σ^* and E_s parameters [Equation (5)], although calculated and experimentally derived ΔG^\ddagger data do not deviate seriously (Table 4).

$$\Delta G^\ddagger(\text{calcd.}) = 30.75\sigma^* - 9.60E_s + 52.2 (r = 0.345, N = 4) \quad (5)$$

The calculated ΔG^\ddagger data depend on the direction of the attack of the reactants. Larger ΔG^\ddagger values were obtained for the reaction of thiane (**29**) if IO_4^- approaches the sulfur atom from the more crowded **A** side rather than from the least crowded **B** side of the molecule (Scheme 4, Table 4, Entries 6 and 7).

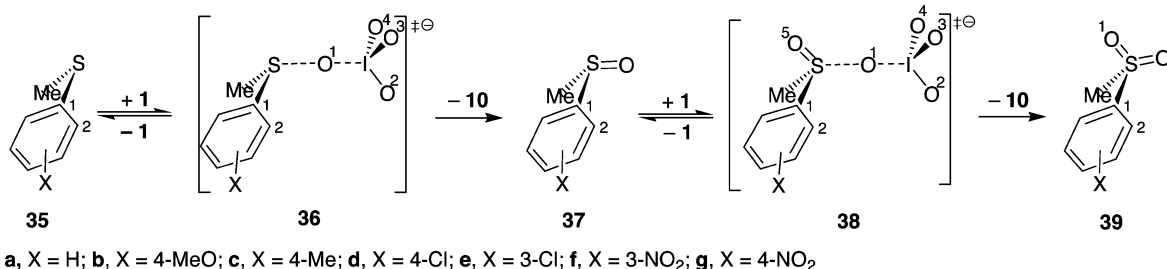
Reactions of Aryl Methyl Sulfides and Methyl Phenyl Sulfoxide with IO_4^-

The structures of the TSs (**36**) for the reactions of aryl methyl sulfides (**35**) with IO_4^- (Scheme 5) are in accord with the oxygen-transfer mechanism [$\theta(\text{MeSO}^1) \approx 90^\circ$, $\theta(\text{C}^1\text{SO}^1) \approx 110^\circ$, $\theta(\text{SO}^1\text{I}) \approx 173^\circ$, $\phi(\text{MeSC}^1\text{C}^2) \approx 14^\circ$, $\phi(\text{O}^1\text{SC}^1\text{C}^2) \approx$

Table 4. Free energies of activation (ΔG^\ddagger), bond lengths (R) and net Mulliken charges (Q) of the TSs (**8**, **30–34**) formed in the oxidation of dialkyl sulfides (**6**, **25–29**) with IO_4^- (**1**, Scheme 1 and Scheme 4). Computations were performed at the DFT(B3LYP)6-31G(d)-SDD level of theory in water at 25 °C. Experimentally derived ΔG^\ddagger data were measured^[11] in 50% (v/v) EtOH/ H_2O at 25 °C.

Reaction	$\Delta G^\ddagger(\text{calcd.})$ [kJ mol^{-1}]	$\Delta G^\ddagger(\text{exp})$ [kJ mol^{-1}]	$R(\text{SO}^1)$ [\AA]	$R(\text{IO}^1)$ [\AA]	$Q(\text{S})$ [a.u.]	$Q(\text{O}^1)$ [a.u.]
1 6 + 1 \rightleftharpoons TS 8	78.2	76.3	2.327	1.977	0.248	−0.685
2 25 + 1 \rightleftharpoons TS 30	69.7	75.4	2.367	1.959	0.217	−0.682
3 26 + 1 \rightleftharpoons TS 31	72.2	76.6	2.373	1.961	0.216	−0.683
4 27 + 1 \rightleftharpoons TS 32	76.4	75.8	2.402	1.952	0.198	−0.679
5 28 + 1 \rightleftharpoons TS 33	77.6	73.9	2.349	1.970	0.207	−0.690
6 29 + 1 \rightleftharpoons TS 34B ^[a]	77.2	75.3	2.355	1.969	0.222	−0.687
7 29 + 1 \rightleftharpoons TS 34A ^[a]	78.8	75.3	2.391	1.960	0.210	−0.681

[a] Attack from the most crowded **A** and from the least crowded **B** sides of thiane (Scheme 4).



Scheme 5. Mechanism for the oxidation of aryl methyl sulfides **35a–35g** and methyl phenyl sulfoxide (**37a**) by IO₄[−] (**1**).

83°; cf. data in Table S5 in the SI]. Later TSs (**36**), with increasing $Q(S)$, $Q(O^1)$ and $R(IO^1)$ and decreasing $R(SO^1)$ values, are formed with increasing electron-withdrawing (e-w) effects and σ constants of the X substituents (Figure 4).

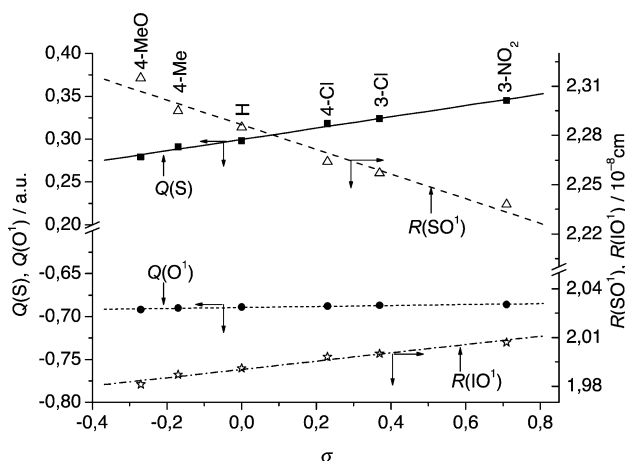


Figure 4. Plots of charges [$Q(S)$, $Q(O^1)$] and bond lengths [$R(SO^1)$, $R(IO^1)$] in TSs **36** against the Hammett σ constants for the reaction of aryl methyl sulfides (XC₆H₄SMe, **35**) with IO₄[−] (**1**; Scheme 5), as calculated at the DFT(B3LYP)/6-31G(d)-SDD level of theory in water at 25 °C. [Correlations: $Q(S) = 0.0660\sigma + 0.300$ ($r = 0.995$); $Q(O^1) = 0.00566\sigma - 0.689$ ($r = 0.959$); $R(SO^1) = -0.075\sigma + 2.287$ ($r = 0.982$); $R(IO^1) = 0.0255\sigma + 1.990$ ($r = 0.985$).]

The experimentally derived ΔG^\ddagger values^[11] [in 50% (v/v) EtOH/H₂O] and the computed ΔG^\ddagger , ΔH^\ddagger and ΔS^\ddagger activation parameters (in water) give linear correlations with the Hammett σ constants (Figure 5). ΔG^\ddagger data decrease with increasing e-d effects of the X substituents as e-d groups accelerate the reaction of sulfides with the periodate ion.^[11] Although the experimentally derived ΔS^\ddagger values were found^[11] to be independent of the substituents of the sulfide [$\Delta S^\ddagger(\text{exp}) \approx -114 \text{ J mol}^{-1} \text{ K}^{-1}$], the computed ΔS^\ddagger data increase with increasing e-w effects of the X groups (Figure 5). This may be the reason for the differences between the slopes of the computed and experimentally derived ΔG^\ddagger versus σ plots.

The rate of reaction of methyl phenyl sulfide (**35a**) and IO₄[−] (**1**) showed a linear dependence^[11] on the Y solvent polarity parameter^[77,78] ($\log k_2 = 0.722Y - 2.575$; $r = 0.998$) in 70:30–30:70 (v/v) EtOH/H₂O mixtures. The data $k_2 = 1.1 \text{ dm}^3 \text{ mol}^{-1} \text{ s}^{-1}$ and $\Delta G^\ddagger = 72.7 \text{ kJ mol}^{-1}$ were obtained by extrapolating the measured rate constants for water ($Y =$

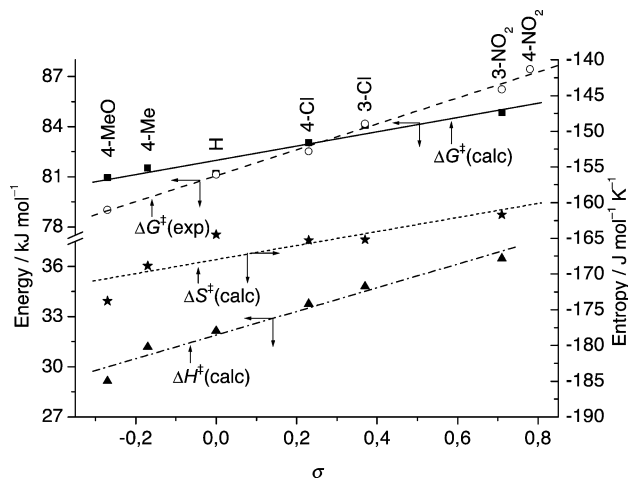


Figure 5. Calculated ΔG^\ddagger , ΔH^\ddagger and ΔS^\ddagger vs. σ and experimentally derived^[11] ΔG^\ddagger vs. σ plots for the reactions of substituted aryl methyl sulfides (XC₆H₄SMe, **35**) with IO₄[−] (**1**; Scheme 5). Calculations were performed at the DFT(B3LYP)/6-31G(d)-SDD level of theory in water at 25 °C. Kinetic measurements were carried out^[11] in 50% (v/v) EtOH/H₂O at 25 °C. [Correlations: $\Delta G^\ddagger(\text{calcd.}) = 4.28\sigma + 82.0$ ($r = 0.961$); $\Delta G^\ddagger(\text{exp}) = 7.77\sigma + 81.1$ ($r = 0.996$); $\Delta H^\ddagger(\text{calcd.}) = 7.07\sigma + 31.9$ ($r = 0.980$); $\Delta S^\ddagger(\text{calcd.}) = 9.82\sigma - 168.0$ ($r = 0.853$). Calculated ΔG^\ddagger , ΔH^\ddagger and ΔS^\ddagger data were obtained by using the parameters of the planar sulfide molecules. $\Delta H^\ddagger(\text{exp}) = 47.2 \text{ kJ mol}^{-1}$ and $\Delta S^\ddagger(\text{exp}) = -113.3 \text{ J mol}^{-1} \text{ K}^{-1}$ for the reaction^[11] of C₆H₅SMe (**35a**) with IO₄[−] (**1**).]

3.493), whereas $\Delta G^\ddagger = 81.2 \text{ kJ mol}^{-1}$ was calculated at the DFT(B3LYP)/6-31G(d)-SDD level of theory in water at 25 °C.

The structural parameters of TS **38a** [$\theta(\text{MeSO}^1) = 96.3^\circ$, $\theta(\text{C}^1\text{SO}^1) = 101.7^\circ$, $\theta(\text{SO}^1\text{I}) = 164.8^\circ$, $\phi(\text{MeSC}^1\text{C}^2) = 100.6^\circ$, $\phi(\text{O}^1\text{SC}^1\text{C}^2) = 160.9^\circ$] and the value $\Delta G^\ddagger = 72.2 \text{ kJ mol}^{-1}$ computed for the oxidation of MeSOPh (**37a**) with IO₄[−] (**1**) to MeSO₂Ph (**39a**) (Scheme 5) are analogous to those obtained for the oxidation of MeSPh (**35a**), which is in agreement with the similar reactivities of sulfides and sulfoxides in oxidations carried out with periodates.^[5–7,10]

Conclusions

Quantum chemical calculations support the suggestion that the oxidation reactions of sulfides and sulfoxides with periodate proceed by a one-step oxygen-transfer mechanism with the simultaneous breaking of the O–I bond and formation of the S=O bond. Other mechanisms, for example, the

attack of the sulfur atom of the substrate on the central iodine atom of the oxidizing agent, can be ruled out.

The sulfide is the electron donor and the periodate is the electron acceptor in the reaction. An uneven charge distribution is developed during the reaction. The attacking oxygen of IO_4^- loses negative charge, whereas the oxygen atoms of the leaving IO_3^- gain negative charge. The structure of the TS is determined by the HOMO–LUMO interaction.

Results can be validated by comparing the computed and experimentally derived ΔG^\ddagger data. ΔG^\ddagger values calculated at the DFT(B3LYP)/6-31G(d)-SDD level of theory were found to be about 10 kJ mol^{-1} higher than data obtained from kinetic measurements. The effect of solvent polarity on ΔG^\ddagger can be computed by using the polarizable continuum model of solvents. On the other hand, the experimentally derived ΔG^\ddagger data depend only slightly on the rearrangement of solvent molecules because changes in the ΔH^\ddagger and ΔS^\ddagger parameters with solvent rearrangement approximately compensate each other.

In accord with the observed pH dependence of the reactions, the calculated relative reactivities of the oxidizing periodate species decrease with hydration and with increasing negative charge on the species. The reactivities of sulfides and sulfoxides in oxidation reactions with IO_4^- are very similar.

The results of computations are in satisfactory agreement with the experimental data. The computations, performed at a moderate level of theory and basis set, rule out certain mechanistic pathways based only on suppositions.

Computational Methods

The geometries of the reactants and transition states were fully optimized without symmetry constraints at the DFT(B3LYP)/6-31G(d) level of theory in water at 25°C by using the Gaussian 03 software package.^[79] The 6-31G(d) basis set was used for all atoms except iodine for which the SDD (Stuttgart/Dresden ECP) was selected with the 6d option because the 6-31G basis set is only applicable up to Kr. For the purpose of validating the chosen level of theory other basis sets and also the MP2 level of theory were tested for the reaction of Me_2S (**6**) and IO_4^- (**1**). MP2 did not prove to be any more accurate than DFT. Nevertheless, of the more than 19 computations performed on the activation barrier of the reaction, the overall results did not reveal any unambiguous trends or better agreement with experiment (Table S7 in the SI) than the moderate DFT(B3LYP)/6-31G(d) level of theory to support the choice of another method or basis set. However, examination of the data obtained with the triple-zeta 6-311 basis set in Table S7 (Entries 10–14) shows that an increasing number of basis functions results in an increase in the barrier height. The average of the data obtained at the computationally demanding TZP level of theory is close to the experimental value and supports our choice of a well-balanced and considerably less expensive DZP basis set, which gives exceptionally good agreement with the experimental data of the studied

reaction. The solvent effect was incorporated by applying the polarizable continuum model^[80] in the integral equation formalism^[81,82] (IEF-PCM) of water. Calculations were made by changing the $\text{S}\cdots\text{O}$ and $\text{S}\cdots\text{I}$ distances of the reactants stepwise to look for TSs and intermediates in the attacks of sulfides on periodates. Structures were checked by vibrational analysis and behaved as energy minima or TSs. No or one imaginary frequency was obtained for reactants and products or TSs, respectively. Selected geometric parameters of the optimized structures obtained by means of DFT computations are listed in Tables S1–S5 and S8 in the SI.

The sums of the electronic and thermal free energies (G) and enthalpies (H) and also the entropies of formation (S) for reactants and TSs were obtained by the standard procedure in the framework of the harmonic approximation^[83,84] and they are listed together with the calculated total energies (E) and numbers of imaginary frequencies in Tables S6 and S7 in the SI. The computed entropy values agree with the data calculated by application of Benson's rule^[85] for the gas phase. As examples, S values of 289.8, 307.0 and $320.5 \text{ J mol}^{-1} \text{ K}^{-1}$ were obtained for Me_2S , Me_2SO and Me_2SO_2 , respectively, by DFT calculations in water at 298 K, and $S = 285.5$, 306.2 and $317.9 \text{ J mol}^{-1} \text{ K}^{-1}$ were calculated on application of Benson's rule. $S = 286.0$ and $310.6 \text{ J mol}^{-1} \text{ K}^{-1}$ were measured^[86] for Me_2S and Me_2SO_2 , respectively, in the gas phase.

The ΔE^\ddagger , ΔG^\ddagger , ΔH^\ddagger and ΔS^\ddagger activation parameters of the reactions were calculated from the differences in the E , G , H and S values (Table S6) of the TSs or calculated data points and the reactants, respectively [Equation (6), $P = E$, G , H or S].

$$\Delta P^\ddagger = P_{\text{TS}} - \sum P_{\text{R}} \quad (6)$$

The values of ΔE^\ddagger , ΔG^\ddagger and ΔH^\ddagger generated were multiplied by 2625.5 to convert them from atomic into kJ mol^{-1} units. Experimentally derived activation parameters for the reactions were calculated from the measured second-order rate constants by using the Eyring equation.^[11] The activation parameters for the reactions of substituted methyl phenyl sulfides were correlated with Hammett σ substituent constants^[87] [Equation (7), $P = G$, H or S], as described previously.^[53–56]

$$\Delta P^\ddagger = \delta \Delta P^\ddagger_\sigma + \Delta P^\ddagger_{\text{O}^\ddagger} \quad (7)$$

The $\delta \Delta P^\ddagger$ reaction constants characterize the effect of substituents on the activation parameters, ΔP^\ddagger and $\Delta P^\ddagger_{\text{O}^\ddagger}$ are the activation parameters of the substituted and unsubstituted compounds, respectively.

Supporting Information (see also the footnote on the first page of this article): Lists of selected atomic charges, bond lengths and angles, torsion angles, calculated total energies, sums of electronic and thermal free energies and enthalpies, entropies of formation and numbers of imaginary frequencies.

Acknowledgments

This work was supported by the Hungarian Scientific Research Foundation and Applied Research Grant of the Hungarian Ministry of Economy and Transport (GVOP) (OTKA No. K 60889 and GVOP-3.1.1-2004-05-0451/3.0).

- [1] G. Dryhurst, *Periodate Oxidation of Diols and other Functional Groups*, Pergamon Press, Oxford, **1970**.
- [2] J. L. Courtney, K. F. Swansborough, *Rev. Pure Appl. Chem.* **1972**, 22, 47–54.
- [3] G. J. Buist, C. Bunton, *J. Chem. Soc. B* **1971**, 2117–2128.
- [4] M. B. Smith, J. March, *March's Advanced Organic Chemistry, Reactions, Mechanism, and Structure*, 5th ed., Wiley, New York, **2001**, p. 1519–1521.
- [5] N. J. Leonard, C. R. Johnson, *J. Org. Chem.* **1962**, 27, 282–284.
- [6] C. R. Johnson, C. McCants, *J. Am. Chem. Soc.* **1965**, 87, 1109–1114.
- [7] B. Sklarz, *Quart. Rev.* **1967**, 21, 3–28.
- [8] C. A. Bunton in *Oxidations in Organic Chemistry* (Ed.: K. B. Wiberg), Academic Press, New York, **1965**, part A, p. 390.
- [9] M. Hudlicky, *Oxidations in Organic Chemistry*, ACS Monograph 180, American Chemical Society, Washington DC, **1990**, p. 265.
- [10] P. Kowalski, K. Mitka, K. Ossowska, Z. Kolarska, *Tetrahedron* **2005**, 61, 1933–1953.
- [11] F. Ruff, Á. Kucsman, *J. Chem. Soc. Perkin Trans. 2* **1985**, 683–687.
- [12] Y. B. Kim, T. Takat, S. Oae, *Tetrahedron Lett.* **1978**, 19, 2305–2308.
- [13] T. Takat, Y. B. Kim, S. Oae, *Bull. Chem. Soc. Jpn.* **1981**, 54, 1443–1447.
- [14] S. Oae, *Organic Sulfur Chemistry: Structure and Mechanism*, CRC Press, Boca Raton, FL, **1991**, p. 198.
- [15] B. J. Evans, J. T. Doi, W. K. Musker, *J. Org. Chem.* **1990**, 55, 2337–2344.
- [16] B. J. Evans, J. T. Doi, W. K. Musker, *J. Org. Chem.* **1990**, 55, 2580–2586.
- [17] S. Oae, *Organic Sulfur Chemistry: Structure and Mechanism*, CRC Press, Boca Raton, FL, **1991**, p. 253–281.
- [18] G. Modena, L. Maioli, *Gazz. Chim. Ital.* **1957**, 87, 1306–1316.
- [19] M. A. D. Dankleff, R. Curci, J. O. Edwards, *J. Am. Chem. Soc.* **1968**, 90, 3209–3218.
- [20] K. Kaczorowska, Z. Kolarska, K. Mitka, P. Kowalski, *Tetrahedron* **2005**, 61, 8315–8327.
- [21] R. Curci, G. Modena, *Tetrahedron* **1966**, 22, 1235–1239.
- [22] R. Curci, F. Di Furia, G. Modena, *J. Chem. Soc. Perkin Trans. 2* **1978**, 603–609.
- [23] S. Campestrini, V. Conte, F. Di Furia, G. Modena, *J. Org. Chem.* **1988**, 53, 5721–5724.
- [24] D. Thenraja, P. Shubramanian, C. Srinivasan, *Tetrahedron* **2002**, 58, 4283–4290.
- [25] K. K. Banerji, *Tetrahedron* **1988**, 44, 2969–2975.
- [26] C. A. Bunton, N. D. Gillitt, *J. Phys. Org. Chem.* **2002**, 15, 29–35.
- [27] R. H. Holm, *Chem. Rev.* **1987**, 87, 1401–1449.
- [28] K. K. Banerji, *J. Chem. Soc. Perkin Trans. 2* **1988**, 2065–2069.
- [29] C. Srinivasan, S. Rajagopal, A. Chellamani, *J. Chem. Soc. Perkin Trans. 2* **1990**, 1839–1843.
- [30] A. Chellamani, P. Kulanthapandi, S. Rajagopal, *J. Org. Chem.* **1999**, 64, 2232–2239.
- [31] R. Sevvil, S. Rajagopal, C. Srinivasan, *J. Org. Chem.* **2000**, 65, 3334–3340.
- [32] V. K. Sivasubramanian, M. Ganesan, S. Rajagopal, R. Ramaraj, *J. Org. Chem.* **2002**, 67, 1506–1514.
- [33] M. Taki, S. Itoh, S. Fukuzumi, *J. Am. Chem. Soc.* **2002**, 124, 998–1002.
- [34] A. Indelli, F. Ferranti, F. Secco, *J. Phys. Chem.* **1966**, 70, 631–636.
- [35] F. Ferranti, A. Indelli, *J. Chem. Soc., Dalton Trans.* **1984**, 1773–1774.
- [36] A. K. Horváth, *J. Phys. Chem. A* **2007**, 111, 890–896.
- [37] G. P. Panigrahi, D. D. Mahapatro, *Int. J. Chem. Kinet.* **1981**, 13, 85–96.
- [38] C. Srinivasan, A. Chellamani, P. Kuthalingam, *J. Org. Chem.* **1982**, 47, 428–431.
- [39] D. G. Lee, T. Chen, *J. Org. Chem.* **1991**, 56, 5346–5348.
- [40] A. Bohra, P. K. Sharma, K. K. Banerji, *J. Org. Chem.* **1997**, 62, 3562–3567.
- [41] K. Rajasekaran, T. Baskaran, C. Gnanasekaran, *J. Chem. Soc. Perkin Trans. 2* **1984**, 1183–1186.
- [42] C. Srinivasan, S. Rajagopal, C. Chellmani, *J. Chem. Soc. Perkin Trans. 2* **1990**, 1839–1843.
- [43] J. B. Barathy, T. K. Ganesan, A. I. M. Sheriff, S. Rajagopal, *Tetrahedron* **1997**, 53, 1131–1144.
- [44] C. Srinivasan, P. Kuthalingam, A. Arumugam, *Can. J. Chem.* **1978**, 56, 3042–3046.
- [45] C. Srinivasan, P. Kuthalingam, A. Arumugam, *J. Chem. Soc. Perkin Trans. 2* **1980**, 170–175.
- [46] L. Ebersson, *Electron Transfer Reactions in Organic Chemistry*, Springer, Berlin, **1987**.
- [47] W. A. Pryor, W. H. Hendricksen Jr., *J. Am. Chem. Soc.* **1983**, 105, 7114–7122.
- [48] J. H. Acquaye, J. G. Muller, K. J. Takeuchi, *Inorg. Chem.* **1993**, 32, 160–165.
- [49] A. Chellamani, N. I. Alhaji, S. Rajagopal, C. Srinivasan, *Tetrahedron* **1995**, 51, 12677–12698.
- [50] A. Chellamani, N. I. Alhaji, S. Rajagopal, *J. Chem. Soc. Perkin Trans. 2* **1997**, 1131–1144.
- [51] T. K. Ganesan, S. Rajagopal, J. B. Bharathy, A. I. M. Sheriff, *J. Org. Chem.* **1998**, 63, 21–26.
- [52] P. Hanson, R. A. A. J. Hendrickx, J. R. L. Smith, *Org. Biomol. Chem.* **2008**, 6, 745–761, 762–771.
- [53] F. Ruff, Ö. Farkas, *J. Org. Chem.* **2006**, 71, 3409–3416.
- [54] F. Ruff, Ö. Farkas, Á. Kucsman, *Eur. J. Org. Chem.* **2006**, 5570–5580.
- [55] F. Ruff, Ö. Farkas, *J. Phys. Org. Chem.* **2008**, 21, 53–61.
- [56] A. Fábián, F. Ruff, Ö. Farkas, *J. Phys. Org. Chem.* **2008**, 21, 988–996.
- [57] C. E. Crouthamel, A. M. Hayes, P. S. Martin, *J. Am. Chem. Soc.* **1951**, 73, 82–87.
- [58] R. M. Kren, H. W. Dodgen, C. J. Nyholm, *Inorg. Chem.* **1968**, 7, 446–451.
- [59] K. Kustin, E. C. Libermean, *J. Phys. Chem.* **1964**, 68, 3969–3973.
- [60] J. E. Taylor, *J. Phys. Org. Chem.* **2007**, 20, 1088–1092.
- [61] F. A. Cotton, G. Wilkinson, *Advanced Inorganic Chemistry*, 3rd ed., Interscience, New York, **1972**, p. 478–481.
- [62] A. J. Downs, C. J. Adams in *Comprehensive Inorganic Chemistry* (Eds.: J. C. Bailar, H. J. Emeleus, R. S. Nyholm, A. F. Trotman-Dickenson), Pergamon Press, Oxford, **1973**, p. 1452–1460.
- [63] G. J. Buist, W. C. P. Hipperson, J. D. Lewis, *J. Chem. Soc. A* **1969**, 307–312.
- [64] G. J. Buist, C. Bunton, W. C. P. Hipperson, *J. Chem. Soc. B* **1971**, 2128–2142.
- [65] N. N. Greenwood, A. Earnshaw, *Chemistry of the Elements*, 2nd ed., Pergamon Press, Oxford, **1997**, p. 1022–1026.
- [66] L. Pauling, *The Nature of the Chemical Bond*, 3rd ed., Cornell University Press, Ithaca, New York, **1960**, p. 164, 189.
- [67] R. S. Berry, S. A. Rice, J. Ross, *Physical Chemistry*, Wiley, New York, **1980**, p. 185.
- [68] J.-W. Chu, B. L. Trout, *J. Am. Chem. Soc.* **2004**, 126, 900–908.
- [69] J. E. Stevens, Q. Cui, K. Morokuma, *J. Chem. Phys.* **1998**, 108, 1544–1551.
- [70] F. C. Grozema, R. W. J. Zijlstra, M. Swart, P. T. v. Duijnen, *Int. J. Quantum Chem.* **1999**, 75, 709–723.
- [71] Y. Inada, K. Akagane, *J. Nucl. Sci. Technol.* **1999**, 34, 217–221.
- [72] F. M. Bickelhaupt, *J. Comput. Chem.* **1999**, 20, 114–128.

- [73] G. T. de Jong, F. M. Bickelhaupt, *ChemPhysChem* **2007**, *8*, 1170–1181.
- [74] L. Pauling, *J. Am. Chem. Soc.* **1947**, *69*, 542–553.
- [75] The TSs **22–24** of the oxygen exchanges (Scheme 3) have only one imaginary mode in which the oxygen atom is transferred between the two equivalent parts of the molecules. The reaction between IO_4^- and IO_3^- has about the same ΔG^\ddagger value as the oxidation of Me_2S with IO_4^- (Table 2, entries 1 and 11). On the other hand, the oxygen exchanges between Me_2S and Me_2SO , as well as between Me_2SO and Me_2SO_2 , would need a much higher free energy of activation (Table 2, Entries 9 and 10).
- [76] R. W. Taft, in: *Steric Effects in Organic Chemistry* (Ed.: M. S. Newman), Wiley, New York, **1956**, p. 632–655.
- [77] E. Grunwald, S. Winstein, *J. Am. Chem. Soc.* **1948**, *70*, 846–854.
- [78] A. H. Fainberg, S. Winstein, *J. Am. Chem. Soc.* **1956**, *78*, 2770–2777.
- [79] M. J. Frisch, G. W. Trucks, H. B. Schlegel, G. E. Scuseria, M. A. Robb, J. R. Cheeseman, J. A. Montgomery Jr., T. Vreven, K. N. Kudin, J. C. Burant, J. M. Millam, S. S. Iyengar, J. Tomasi, V. Barone, B. Mennucci, M. Cossi, G. Scalmani, N. Rega, G. A. Peterson, H. Nakatsuji, M. Hada, M. Ehara, K. Toyota, R. Fukuda, J. Hasegawa, M. Ishida, T. Nakajima, Y. Honda, O. Kitao, H. Nakai, M. Klene, X. Li, J. E. Knox, H. P. Hartchian, J. B. Cross, C. Adamo, C. Jaramillo, R. Gomperts, R. E. Stratmann, O. Yazyev, A. J. Austin, R. Cammi, C. Pomelli, J. W. Ochterski, P. Y. Ayala, K. Morokuma, G. A. Voth, P. Salvador, J. J. Dannenberg, V. G. Zakrzewski, S. Dapprich, A. D. Daniels, M. C. Strain, Ö. Farkas, D. K. Malick, A. D. Rabuck, K. Raghavachari, J. B. Foresman, J. V. Ortiz, Q. Cui, A. G. Baboul, S. Clifford, J. Cioslowski, B. B. Stefanov, G. Liu, A. Liashenko, P. Piskorz, I. Komáromi, R. L. Martin, D. J. Fox, T. Keith, L. A. Al-Laham, C. Y. Peng, A. Nanayakkara, M. Challacombe, P. M. W. Gill, B. Johnson, W. Chen, M. W. Wong, C. Gonzalez, J. A. Pople, *Gaussian 03*, Revision C.02, Gaussian Inc., Pittsburg, PA, **2003**.
- [80] J. Tomasi, M. Persico, *Chem. Rev.* **1994**, *94*, 2027–2094.
- [81] E. Cancès, B. Mennucci, *J. Chem. Phys.* **2001**, *114*, 4744–4745.
- [82] D. M. Chipman, *J. Chem. Phys.* **2000**, *112*, 5558–5565.
- [83] D. A. McQuarrie, J. D. Simon, *Molecular Thermodynamics*, University Science Books, Sausalito, CA, **1999**.
- [84] http://www.gaussian.com/g_whitepap/thermo/thermo.pdf.
- [85] S. W. Benson, *Thermochemical Kinetics*, Wiley, New York, **1976**, p. 19–72.
- [86] D. R. Lide (Ed.), *CRC Handbook of Chemistry and Physics*, CRC Press, Boca Raton, FL, **1995**, chapter 5–4.
- [87] C. Hansch, H. Leo, R. W. Taft, *Chem. Rev.* **1991**, *91*, 165–195.

Received: November 27, 2008
Published Online: March 18, 2009